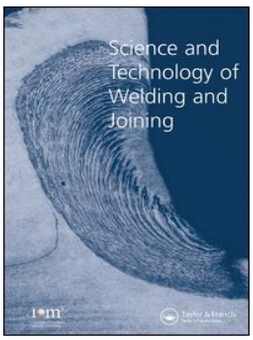

Science and Technology of Welding and Joining

ISSN: 1362-1718 (Print) 1743-2936 (Online) Journal homepage: https://www.tandfonline.com/loi/ystw20

Influence of Zn coating on friction stir spot welded magnesium-aluminium joint

R. Z. Xu, D. R. Ni, Q. Yang, C. Z. Liu & Z. Y. Ma

To cite this article: R. Z. Xu, D. R. Ni, Q. Yang, C. Z. Liu & Z. Y. Ma (2017) Influence of Zn coating on friction stir spot welded magnesium-aluminium joint, Science and Technology of Welding and Joining, 22:6, 512-519, DOI: 10.1080/13621718.2016.1266735

To link to this article: https://doi.org/10.1080/13621718.2016.1266735

SCIENCE AND TECHNOLOGY OF WELDING AND JOINING, 2017
VOL. 22, NO. 6, 512–519
http://dx.doi.org/10.1080/13621718.2016.1266735

The Institute of Materials, Minerals and Mining

Taylor & Francis
Taylor & Francis Group

Influence of Zn coating on friction stir spot welded magnesium-aluminium joint

R. Z. Xu[a,b], D. R. Ni[a], Q. Yang[a], C. Z. Liu[b] and Z. Y. Ma[a]

[a]Shenyang National Laboratory for Materials Science, Institute of Metal Research, Chinese Academy of Sciences, Shenyang, China; [b]College of Material Science and Engineering, Shenyang Aerospace University, Shenyang, China

ABSTRACT

For friction stir spot welded (FSSW) magnesium–aluminium joints, the formation of Mg–Al intermetallics in the hook region and cracking at the interface damaged seriously the strength of Mg–Al joints, resulting in lower joint load of only 0.8 ± 0.2 kN. When adding the hot-dipped Zn coating on the Al substrate surface prior to FSSW, a brazed layer, composed of Mg–Zn and Al–Zn diffusion zones at the edge of the shoulder, and a transition layer, composed of $MgZn_2$, Zn-rich zone and residual Zn in the hook region, were formed in the FSSW Mg–Al joint, eliminating the cracking and Mg–Al intermetallics in the FSSW joint without the Zn coating. The load of the joint with the Zn coating increased to 3.7 ± 0.3 kN.

ARTICLE HISTORY
Received 22 September 2016
Accepted 24 November 2016

KEYWORDS
Friction stir spot welding; dissimilar metals; hot-dipped Zn coating; intermetallic compound

Introduction

In order to increase fuel efficiency and reduce anthropogenic climate-changing and pollution, various industries, especially automotive and aerospace, have a pressing need for structural lightweight. Al and its alloys, as good lightweight materials, have been widely used in the transportation industry owing to the good ductility, formability and thermal conductivity [1,2]. In addition, ultra-lightweight Mg alloys have increasingly been used in the vehicle fabrication due to the lower density, higher specific stiffness and strength, excellent stability of size and acceptable process ability [3,4]. The structural application of Mg alloys inevitably involves the joining and welding of Mg and Al alloys [5,6].

During the welding of Mg–Al dissimilar metals, such as vacuum diffusion bonding [7], laser welding [8], explosive welding [9], and friction stir welding (FSW) [5,6], the Mg–Al intermetallic compounds (IMCs) with a very high hardness and brittleness were easily formed at the interface. These IMCs preferentially act as the source of micro-cracks in mechanical property tests, and then deteriorate the mechanical property of the joint. Therefore, eliminating or reducing the effect of IMCs on the joint strength is the focus of Mg–Al dissimilar metals welding [10].

Spot welding is a widely used and important welding process in the field of automotive industry. Friction stir spot welding (FSSW) is a variant of FSW [11,12]. As a solid state joining method, FSSW presents a great potential in substituting conventional resistance spot welding and riveting in joining lightweight structural metals for the automotive and aerospace industries [13,14]. However, many studies have indicated that the formation of IMCs in the weld centre and small bonded area in the FSSW Mg–Al joints seriously reduced the joint properties [15–18].

Some work focused on reducing the formation of IMCs by optimising the welding parameters, such as rotation rate, duration time and plunge depth, however, this could not eliminate the Mg–Al IMCs [6,15,19]. Furthermore, some studies tried to increase the bonded area and the nugget size by using the improved FSSW processes, such as bonding-FSSW [20] and preheating-FSSW [21]. For bonding-FSSW, the area of the bonded zone of the joint was increased by adhesives, so the load of the joint could be improved. However, the aging and poor high-temperature performance of adhesives should not be ignored. For the preheating-FSSW, the width of the bonded zone was increased because the welding samples were heated to 473 K by resistance heating rods before welding. However, the troublesome operation would limit the wide applications of this process. In addition, the above two hybrid technologies only increased the area of the bonding zone, but could not avoid the appearance of Mg–Al IMCs.

For other welding processes, adding metal interlayer is an important way of reducing the formation of IMCs, such as resistance spot welding with a Zn coated steel interlayer [22] or Zn interlayer [23], forge welding with a Cu, Ni, or Ti interlayer [24], laser welding with a

CONTACT Z. Y. Ma zyma@imr.ac.cn Shenyang National Laboratory for Materials Science, Institute of Metal Research, Chinese Academy of Sciences, 72 Wenhua Road, Shenyang110016, China

Ti interlayer [25], diffusion welding with a Zn interlayer [26], pre-roll-assisted A-TIG welding with a Zn interlayer [27] and ultrasonic spot welding with a Sn interlayer [28]. However, for Mg–Al FSSW, welding temperature is not high, so the insertion of metal layer with low melting point between the Mg and Al sheets is a more promising way of mitigating the formation of undesirable IMCs.

According to the Mg–Zn and Al–Zn phase diagrams, Zn could react with Mg at a low temperature, forming the Mg–Zn IMCs. In addition, a large solid solubility could be formed between Zn and Al. Therefore Zn may act as an alloying element to improve the mechanical properties of the FSSW Mg–Al joint. However, the reaction between Zn interlayer and Al substrate would be very difficult due to the oxide film of Al surface.

In order to promote the alloying between Al and Mg, a Zn interlayer is prepared by hot-dipped galvanising in this study. The influencing mechanism of the hot-dipped Zn coating addition on the microstructure and mechanical property of the FSSW joint of Mg and Al was investigated in detail.

Experimental

The substrate material used in the present study was 2.4 mm thick sheet of AZ31 Mg alloy with a composition of Mg–3.0Al–0.8Zn–0.3Mn–0.01Si (wt-%) and 1.5 mm thick sheet of 2024 Al alloy with a composition of Al–4.0Cu–0.5Mn (wt-%). Prior to the welding, Al alloy sheets were first degreased by the alcohol. After fluxing and preheating treatments, coupons were hot-dipped into a molten bath consisting of Zn with the purities of 99.9 wt-%. The temperature of the molten bath was set at 450°C. A molten salt furnace was used to maintain the temperature during the dipping process. The schematics of Mg–Al FSSW without and with the Zn coating are shown in Figure 1. AZ31 specimen was lapped on the top of 2024 specimen by a holding fixture.

All the FSSW operations with and without the coating were conducted at a tool rotation rate of 3000 rev min^{-1} and a plunge rate of 2.5 mm s^{-1} using a tool with a shoulder 12 mm in diameter and a taper threaded pin 3.1 mm in length and 5 mm in root diameter. The tool withdrawing rate was 30 mm s^{-1} at the end of each spot welding operation and the dwell time was 5 s.

Specimens for microstructure examinations were sectioned through the centre of the joint and parallel to the loading direction. After being mechanically ground and polished, the specimens were etched with an etching reagent consisting of 4.2 g picric acid, 10 mL acetic acid, 10 mL H_2O and 70 mL ethanol. Microstructures were examined by optical microscope (OM), scanning electron microscope (SEM, LEO Supra 35) with an energy-dispersive X-ray dispersive spectrometer (EDS, Oxford Instruments X-Max) and transmission electron microscope (TEM, FEI Tecnai F20) equipped with an energy-dispersive X-ray spectrometer (EDS, Oxford Instruments INCA).

The lap-shear specimens with a length of 100 mm, a width of 25 mm and a 25 × 25 mm overlap area were electrical discharge machined from the FSSW joints. The lap-shear tensile tests were conducted using a Zwick/Roell Z050 tester at a tensile speed of 0.5 mm/min. The property values for each condition were calculated by averaging three test results. The fracture location and characteristics were examined using OM and SEM.

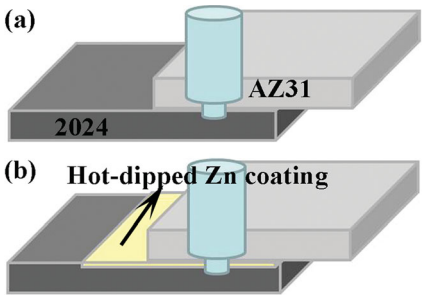

Figure 1. Schematic of AZ31-2024 dissimilar metal FSSW (a) without and (b) with the addition of hot-dipped Zn coating.

Results

FSSW of Mg alloy and Al alloy dissimilar metals without Zn coating

Macrostructure and microstructure of FSSW Mg–Al joint

Figure 2 shows the typical cross-section photograph of the FSSW Mg–Al joint without Zn coating. AZ31 Mg alloy sheet and 2024 Al alloy sheet were successfully joined by FSSW. The magnified microstructures (Figure 3(a)) of bonded zone on the advancing side (AS) exhibited that an obvious transition zone about 4 μm in thickness (Figure 3(b)) was formed at the interface due to the diffusion reaction of Mg substrate and Al substrate. The elemental analysis of line D in Figure 3(b) revealed the mutual presence of Al and Mg across the reaction layer as shown in Figure 3(d), suggesting that the IMC layer formed at the Al/Mg interface during FSSW.

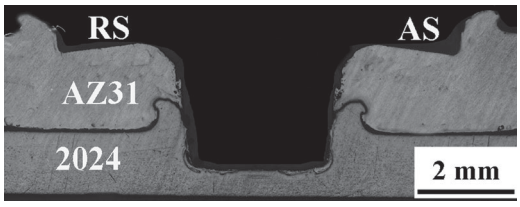

Figure 2. Typical cross-section photograph of FSSW AZ31-2024 joint without Zn coating.

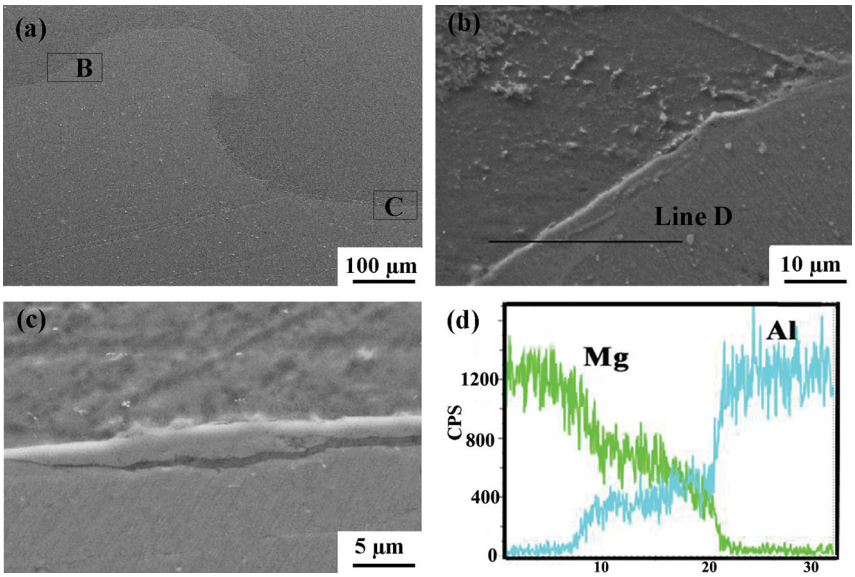

Figure 3. (a) SEM photograph of advanced side in FSSW AZ31-2024 joint and magnified views of (b) region B and (c) region C in Figure 3(a); (d) elemental analysis of line D in Figure 3(b).

In addition, an obvious transition zone was also detected at the edge of hook region (zone C in Figure 3(a)) in the FSSW joint, but it did not form an effective bonding zone due to the occurrence of cracking at the Mg–Al interface as shown in Figure 3(c).

Properties and fracture characteristic of Mg–Al joint

The tensile-shear testing showed that the load of joint was only 0.8 ± 0.2 kN. Figure 4(a) shows the typical fracture location of the FSSW Mg–Al joint. It is found that the fracture of the joint occurred along the interface between AZ31 Mg alloy and 2024 Al alloy. Figure 4(b) shows the SEM micrograph of the fracture surface of the Mg–Al joint on the Al substrate side. It can be seen that fracture surface was quite smooth, suggesting the brittle fracture characteristics of the joint.

In short, the formation of IMC at the Mg–Al interface and small bonding area in the FSSW Mg–Al joint deteriorate seriously the load of joint.

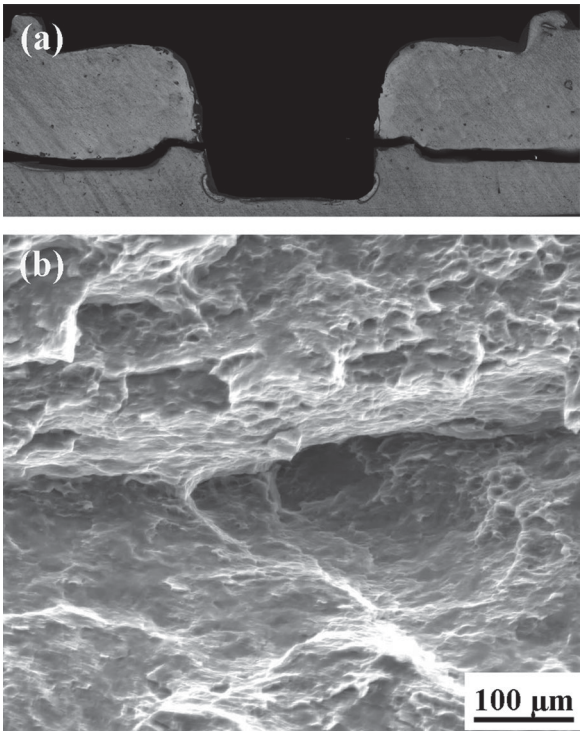

Figure 4. (a) Typical fracture location and (b) surface microstructure of FSSW AZ31-2024 joint.

FSSW of Mg alloy and Al alloy dissimilar metals with a hot-dipped Zn coating

Characteristics of Zn coating on the Al substrate surface

Figure 5(a,b) shows the cross-section photograph of the hot-dipped Zn coating on the Al substrate and elemental analysis of line B in Figure 5(a), respectively. It can be seen that the coating had a thickness of about 50 μm and was almost completely composed of Zn with a small quantity of Al diffusing into the Zn coating.

Macrostructure and microstructure of FSSW Mg–Al joint with Zn coating

Figure 6(a) shows the typical cross-section photograph of the FSSW Mg–Al joint with the addition of hot-dipped Zn coating. It is clear that Mg alloy sheet and Al alloy sheet were well joined together. The magnified microstructures (Figure 6(b,c)) of regions B and C in Figure 6(a) showed the formation of an obvious transition zone at the interface due to the diffusion reaction of Zn coating and substrates. The continuous reaction layer was very thin at the keyhole periphery (Figure 6(b) and Figure 7(a)). The representative line analysis of Mg, Zn and Al cross the interface is shown in Figure 7(b). It was found that Zn was enriched at the Mg–Al interface. The Zn-rich layer was so thin that the EDS result was

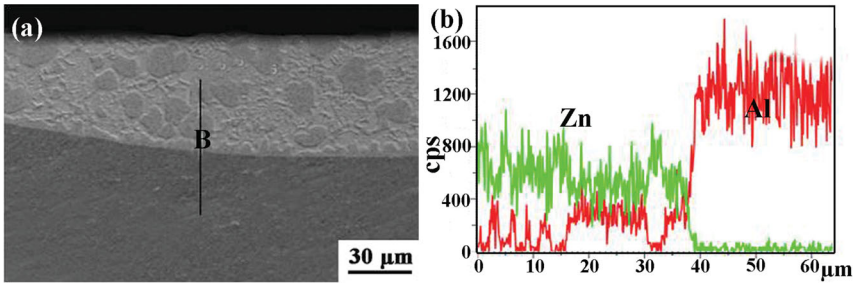

Figure 5. (a) Typical cross-section photograph of Zn coating on the Al substrate surface and (b) elemental analysis of line B in Figure 5(a).

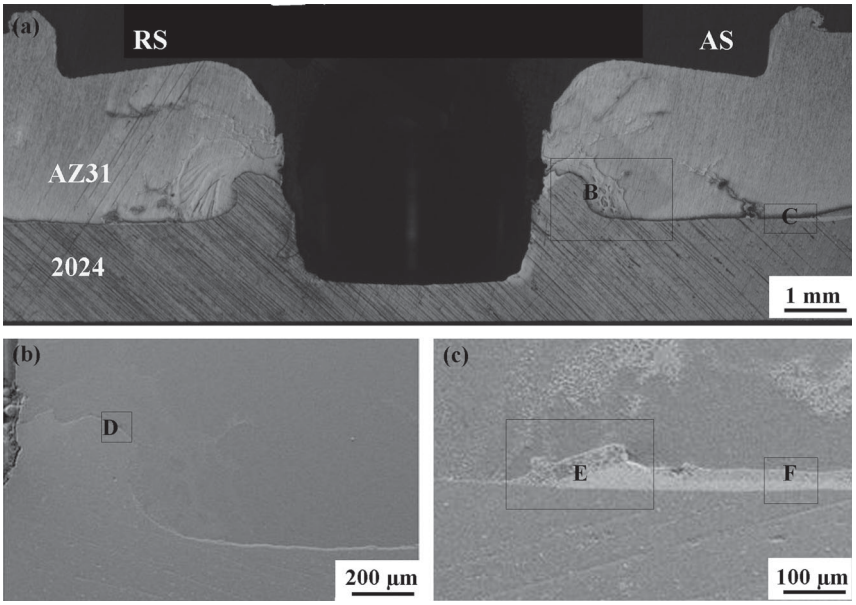

Figure 6. (a) Typical cross-section photograph of FSSW AZ31-2024 joint with Zn coating and the microstructures of (b) region B and (c) region C in (a).

not accurate to reflect its thickness and identify the IMC phase.

The thickness of the reaction layer increased obviously at the edge of FSSW joint (Figure 6(c)). The magnified microstructures of regions E and F in Figure 6(c) exhibited that the reaction layer could be divided mainly into two typical diffusion zones as shown in Figure 8(a,b). The EDS line analysis results shown in Figure 8(c,d) revealed that Mg–Zn and Zn–Al diffusion zones formed at the interface, preventing the inter-diffusion of Mg and Al substrate.

The typical microstructures of interface (region D of Figure 6(b)) on the Mg side and Al side are shown in Figure 9(a,b), respectively. There were no Mg–Al IMCs at the interface between AZ31 Mg alloy and 2024 Al alloy. $MgZn_2$ was detected next to the Mg side (Figure 9(a)) and the residual Zn and Zn-rich zone were found next to the Al side (Figure 9(b)). High-resolution TEM (HRTEM) examinations on the Zn-rich zone indicated that a large number of acicular strips and fine particles were distributed in the Zn-rich zone as shown in Figure 10(a,b). The acicular and granular structure may be Al-rich phase and β-Zn phase, respectively.

In short, hot-dipped Zn coating on the Al substrate surface impeded the formation of Mg–Al IMCs and increased obviously the bonding area of FSSW joint.

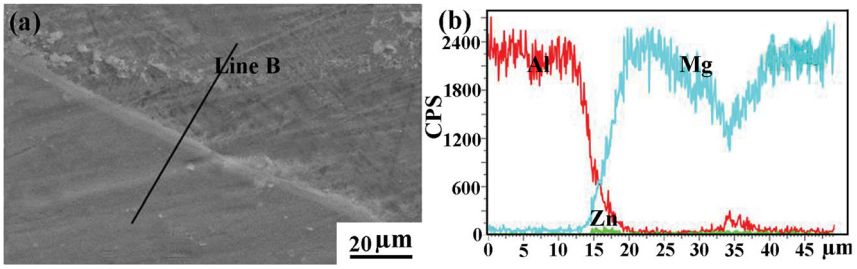

Figure 7. (a) Magnified microstructure of region D in Figure 6(b) and (b) elemental analysis of line B in Figure 7(a).

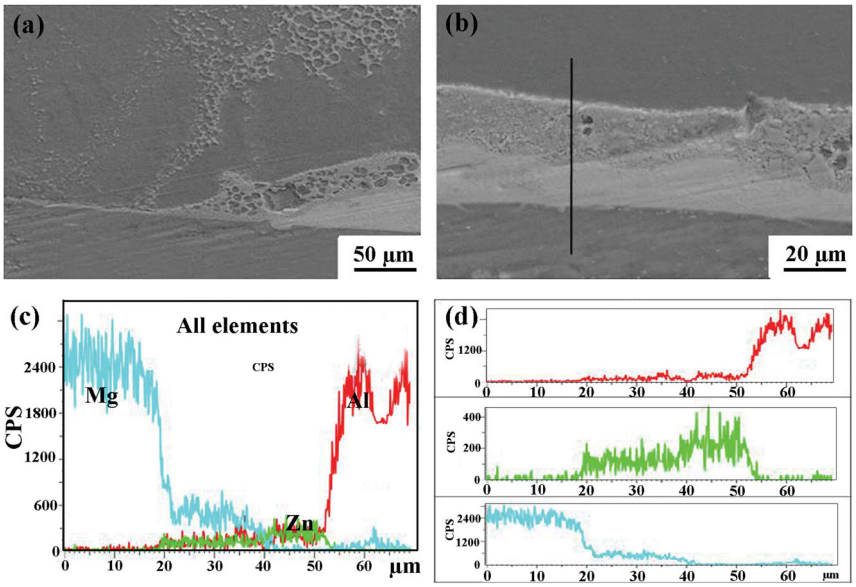

Figure 8. Magnified microstructures of (a) region E and (b) region F in Figure 6(c); elemental line analysis: (c) comprehensive and (d) individual analysis.

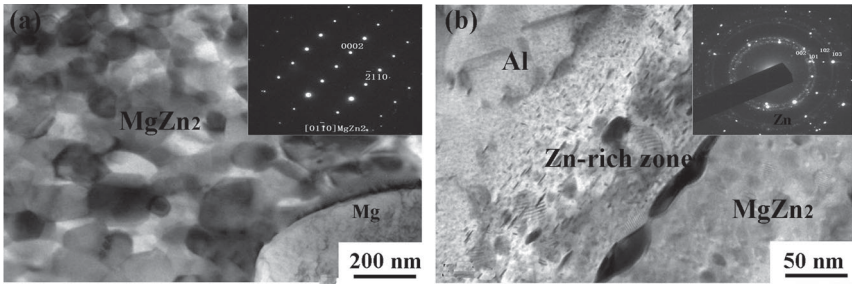

Figure 9. TEM images showing interfacial microstructures (region D in Figure 6(b)): (a) Mg side and (b) Al side.

Properties and fracture characteristic of Mg–Al joint with Zn coating

The tensile-shear testing showed that the load of joint could reach 3.7 ± 0.3 kN, which is superior to that of other Mg–Al joints prepared under a variety of FSSW conditions as shown in Table 1 [6,15,18–21].

Figure 11(a) shows the typical fracture location of Mg–Al joint with the Zn coating. It could be seen that the fracture of the joint occurred along the Mg–Al interface. Magnified photograph showed that the fracture initiated from the IMCs rather than the hook region (Figure 11(c)), and then propagated along the transition zone (Figure 11(a,b)).The fracture mode is different from that of the FSSW Mg–Al joint without the Zn coating.

Discussion

Influence of Zn coating on the microstructure evolution of FSSW Mg–Al joint

During Mg–Al FSSW with the addition of the Zn coating, the microstructure and phases of welded joint was closely related to the reaction among the Zn coating,

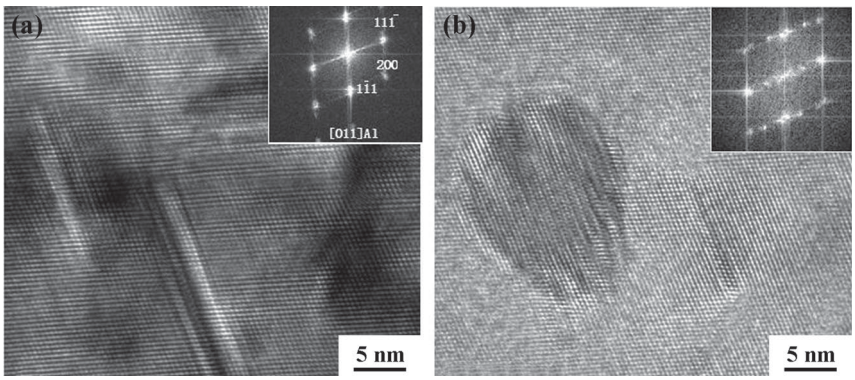

Figure 10. HRTEM images of Zn-rich zone: (a) acicular structure and (b) granular structure.

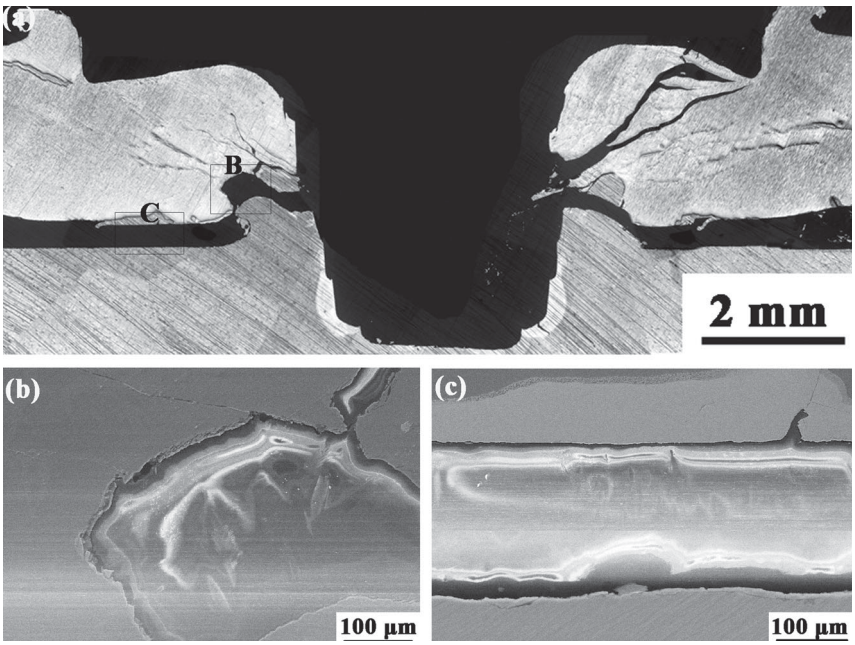

Figure 11. (a) Typical fracture location of FSSW AZ31-2024 joint with Zn coating and magnified photographs of region B and (b) region C in Figure 11(a).

Table 1. A summary of tensile-shear data for various FSSW Mg–Al joints prepared under a variety of FSSW conditions.

FSSW joint	Shoulder diameter, or hybrid process	Load (kN)	Ref.
AZ31-5083	10.0 mm, FSSW	1.5	[15]
AZ31-5754	13.0 mm, FSSW	~ 1.0	[18]
AZ31-6k21	13.5 mm, FSSW	1.6	[6]
AM60-6022	12.0 mm, FSSW	2.5	[19]
AZ31-5774	13.0 mm, FSSW	~ 1.5	[20]
AZ31-6061	10.0 mm, FSSW	1.7 ± 0.34	[21]
6061-AZ31	10.0 mm, FSSW	1.4 ± 0.25	[21]
AZ31-6061	10.0 mm, FSSW + Preheating	2.0 ± 0.23	[21]
6061-AZ31	10.0 mm, FSSW + Preheating	1.2 ± 0.29	[21]

AZ31 Mg substrate and 2024 Al substrate under the action of the stir tool. The hot-dipped Zn coating of various zones had different reactions with the Mg and Al substrates due to the differences in material flow and heat input.

The Zn coating underneath the stir pin was broken first and then moved towards the pin root together with the Al substrate underneath the shoulder. Therefore the Zn coating in this zone had little effect on the microstructure of Mg–Al interface due to the disruption of Zn coating.

The Zn coating underneath the shoulder can be divided into two zones. In the zone adjacent to the keyhole, the Zn coating was heated and softened, and then moved upwards together with the Al substrate. At the same time, the diffusion reaction between the Zn coating and the substrates occurred in this zone (Figures 6(b) and 7(a)). The inter-diffusion of Mg and Al substrates was impeded by the $MgZn_2$, Zn-rich zone and residual Zn (Figures 9 and 10).

In the zone under the edge of the shoulder, the Zn coating almost did not move, but could form a brazed bonding with the substrates as shown in Figure 6(a,c). During FSSW, the Zn coating could react with the substrates to form a good bonding layer composed of Mg–Zn and Zn–Al diffusion zones (Figure 6(c) and Figure 8) due to the heat and pressure produced by the stir tool, realising the brazing joining of Mg and Al substrates in this zone.

According to the above analysis, a schematic of the microstructure evolution of the joints with the hot-dipped Zn coating is provided in Figure 12. Under the action of the plunge, rotation, and dwelling of the stir tool, the joint could be divided mainly into three typical parts, i.e. zones I, II and III as shown in Figure 12(a,b).

In zone I, the reaction temperature was higher than that of other zones, but a keyhole through the interface remained after drawing the stir pin and destroyed the bonding of Mg and Al substrates (Figure 12(b)). Therefore, the Zn coating had a slight effect on the interface reaction between Mg and Al substrates in this zone.

In zone II, on the one hand, the most of Zn coating diffused into the Mg substrate, resulting in that the thickness of Zn coating was reduced obviously; on the other hand, a small quantity of Zn coating on the Al substrate surface played a role in eliminating the formation of Mg–Al IMCs, realising the bonding of AZ31 Mg alloy and 2024 Al alloy in this zone (Figure 12(b)).

In zone III, the diffusion of Zn coating and Mg substrate took place due to the action of the shoulder. At the same time, the Zn coating and Al substrate further diffused into each other during FSSW. As a result, brazed bonding zone was formed in this zone (Figure 12(c)).

At last, the Zn coating reacted with the Mg and Al substrates, avoiding the formation of Mg–Al brittle IMCs, increasing the bonding area during FSSW (Figure 12(d)).

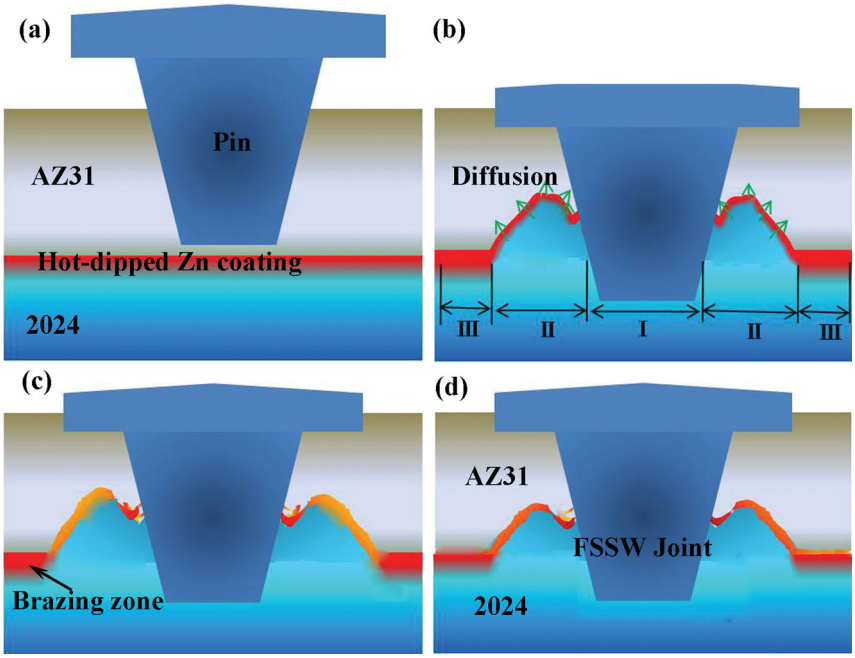

Figure 12. Schematic of microstructure evolution of typical FSSW joint with Zn coating: (a) lap construction, (b) three zones of joint and movement of Zn coating, (c) formation of brazed zone and (d) sound FSSW joint.

Relationship between microstructure and mechanical property

For the FSSW Mg–Al joint without the addition of Zn coating, the crack initiated from the cracking (Figure 3(c)) and grew from the tip of the hook to the keyhole periphery in tensile-shear testing, leading to the failure of joint (Figure 4). On the one hand, the cracking led to the decline of effective bonding area; on the other hand, the Mg–Al IMCs at the interface in the hook region is very brittle. Therefore, the load of Mg–Al joint without the addition of Zn coating is very low (only 0.8 ± 0.2 kN).

For the FSSW Mg–Al join with the addition of Zn coating, the Zn coating promoted the formation of a brazed zone (zone III) and eliminated the brittle Mg–Al IMCs of hook region (Figures 5–10). In tensile-shear testing, the crack initiated from the brazed zone composed of Mg–Zn and Zn–Al diffusion zones and then propagated through the interface zone composed of $MgZn_2$, Zn-rich zone and residual Zn (zone II) as show in Figure 11. Therefore, the formation of the brazed zone (zone III) significantly increased the area of the bonded zone of the joints, thereby increasing the joint load (3.7 ± 0.3 kN).

Conclusions

In this study, the effect of adding hot-dipped Zn coating on the microstructural features and properties of the FSSW Mg–Al joint was investigated. The following conclusions were drawn.

(1) For the FSSW joint without the addition of Zn coating, the formation of brittle Mg–Al IMCs in the hook region and cracking at the interface at the edge zone of joint damaged seriously the strength of the joint. The load of the joint is only 0.8 ± 0.2 kN.

(2) Adding the Zn coating on the Al substrate surface prior to FSSW could lead to the formation of a brazed layer composed of Mg–Zn and Al–Zn diffusion zones at the edge of shoulder and a transition zone composed of $MgZn_2$, Zn-rich zone and residual Zn in the hook region, eliminating the cracking and Mg–Al IMCs in the FSSW Mg–Al joint without the Zn coating.

(3) For the joint with the addition of the Zn coating, the crack initiated from the brazed zone composed of Mg–Zn and Zn–Al diffusion zones and then propagated through the interface in the hook region. The load of the joint could reach 3.7 ± 0.3 kN, which is far higher than that of the joint without the addition of the Zn coating.

Disclosure statement

No potential conflict of interest was reported by the authors.

Funding

This study was supported by the National Natural Science Foundation of China under Grant Nos. 51601121, 51371179 and 51331008, and Natural Science Foundation of Liaoning Province No. L201624 and 201602570.

References

[1] Qiu RF, Iwamoto C, Satonaka S. The influence of reaction layer on the strength of aluminum/steel joint welded by resistance spot welding. Mater Character. 2009;60:156–159.

[2] Hajjari E, Divandari M, Razavi SH, et al. Intermetallic compounds and antiphase domains in Al/Mg compound casting. Intermetallics. 2012;23:182–186.
[3] Yang J, Ni DR, Wang D, et al. Strain-controlled low-cycle fatigue behavior of friction stir-welded AZ31 magnesium alloy. Metall Mater Trans A. 2014;45:2101–2115.
[4] Yang J, Wang D, Xiao BL, et al. Effects of rotation rates on microstructure, mechanical properties, and fracture behavior of friction stir-welded (FSW) AZ31 magnesium alloy. Metall Mater Trans A. 2013;44:517–530.
[5] Kostka A, Coelho RS, dos Santos J, et al. Microstructure of friction stir welding of aluminium alloy to magnesium alloy. Scr Mater. 2009;60:953–956.
[6] Choi D, Ahn B, Lee C, et al. Formation of intermetallic compounds in Al and Mg alloy interface during friction stir spot welding. Intermetallics. 2011;19:125–130.
[7] Peng L, Yajiang L, Haoran G, et al. A study of phase constitution near the interface of Mg/Al vacuum diffusion bonding. Mater Lett. 2005;59:2001–2005.
[8] Borrisutthekul R, Miyashita Y, Mutoh Y. Dissimilar material laser welding between magnesium alloy AZ31B and aluminum alloy A5052-O. Sci Technol Adv Mater. 2005;6:199–204.
[9] Yana YB, Zhang ZW, Shen W, et al. Microstructure and properties of magnesium AZ31B-aluminum 7075 explosively welded composite plate. Mater Sci Eng A. 2010;527:2241–2245.
[10] Li XR, Liang W, Zhao XG, et al. Bonding of Mg and Al with Mg–Al eutectic alloy and its application in aluminum coating on magnesium. J Alloys Compds. 2009;471:408–411.
[11] Lathabai S, Painter MJ, Cantin GMD, et al. Friction spot joining of an extruded Al–Mg–Si alloy. Scr Mater. 2006;55:899–902.
[12] Gerlich A, Su P, North TH. Tool penetration during friction stir spot welding of Al and Mg alloys. J Mater Sci. 2005;40:6473–6481.
[13] Bilici MK, Yukler AI, Kurtulmus M. The optimization of welding parameters for friction stir spot welding of high density polyethylene sheets. Mater Des. 2011;32:4074–079.
[14] Rodrigues DM, Loureiro A, Leitao C, et al. Influence of friction stir welding parameters on the microstructural and mechanical properties of AA 6016-T4 thin welds. Mater Des. 2009;30:1913–1921.
[15] Sato Y, Shiota A, Kokawa H, et al. Effect of interfacial microstructure on lap shear strength of friction stir spot weld of aluminium alloy to magnesium alloy. Sci Technol Weld Join. 2010;15:319–324.
[16] Gerlich A, Su P, North T. Peak temperatures and microstructures in aluminium and magnesium alloy friction stir spot welds. Sci Technol Weld Join. 2005;10:647–652.
[17] Suhuddin UFH, Fischer V, dos Santos JF. The thermal cycle during the dissimilar friction spot welding of aluminum and magnesium alloy. Scr Mater. 2013;68:87–90.
[18] Chowdhury SH, Chen DL, Bhole SD, et al. Lap shear strength and fatigue life of friction stir spot welded AZ31 magnesium and 5754 aluminum alloys. Mater Sci Eng A. 2012;556:500–509.
[19] Rao HM, Yuan W, Badarinarayan H. Effect of process parameters on mechanical properties of friction stir spot welded magnesium to aluminum alloys. Mater Des. 2015;66:235–245.
[20] Chowdhur SH, Chen DL, Bhole SD, et al. Lap shear strength and fatigue behavior of friction stir spot welded dissimilar magnesium-to-aluminum joints with adhesive. Mater Sci Eng A. 2013;562:53–60.
[21] Shen J, Li Y, Zhang T, et al. Preheating friction stir spot welding of Mg/Al alloys in various lap configurations. Sci Technol Weld Join. 2015;20:1–10.
[22] Penner P, Liu L, Gerlich A, et al. Dissimilar resistance spot welding of aluminum to magnesium with Zn coated steel interlayers. Mater Des. 2014;93:225–231.
[23] Zhang Y, Luo Z, Li Y, et al. Microstructure characterization and tensile properties of Mg/Al dissimilar joints manufactured by thermo-compensated resistance spot welding with Zn interlayer. Mater Des. 2015;75:166–173.
[24] Yamagishi H, Sumioka J, Kakiuchi S, et al. Forge welding of magnesium alloy to aluminum alloy using a Cu, Ni, or Ti interlayer. Metall Mater Trans A. 2015;46:3601–3611.
[25] Gao M, Mei SW, Li XY, et al. Characterization and formation mechanism of laser-welded Mg and Al alloys using Ti interlayer. Scr Mater. 2012;67:193–196.
[26] Zhao LM, Zhang ZD. Effect of Zn alloy interlayer on interface microstructure and strength of diffusion-bonded Mg–Al joints. Scr Mater. 2008;58:283–286.
[27] Zhang HT, Dai XY, Feng JC. Joining of aluminum and magnesium via pre-roll-assisted A-TIG welding with Zn interlayer. Mater Lett. 2014;122:49–51.
[28] Patel VK, Chen DL, Bhole SD. Dissimilar ultrasonic spot welding of Mg–Al and Mg-high strength low alloy steel. Theor Appl Mech Lett. 2014;4:041005-1–041005-8.